



## Manufacturing & Service Operations Management

Publication details, including instructions for authors and subscription information:  
<http://pubsonline.informs.org>

### Modeling Influenza Pandemic and Planning Food Distribution

Ali Ekici, Pınar Keskinocak, Julie L. Swann

To cite this article:

Ali Ekici, Pınar Keskinocak, Julie L. Swann (2014) Modeling Influenza Pandemic and Planning Food Distribution. *Manufacturing & Service Operations Management* 16(1):11-27. <http://dx.doi.org/10.1287/msom.2013.0460>

Full terms and conditions of use: <http://pubsonline.informs.org/page/terms-and-conditions>

This article may be used only for the purposes of research, teaching, and/or private study. Commercial use or systematic downloading (by robots or other automatic processes) is prohibited without explicit Publisher approval, unless otherwise noted. For more information, contact [permissions@informs.org](mailto:permissions@informs.org).

The Publisher does not warrant or guarantee the article's accuracy, completeness, merchantability, fitness for a particular purpose, or non-infringement. Descriptions of, or references to, products or publications, or inclusion of an advertisement in this article, neither constitutes nor implies a guarantee, endorsement, or support of claims made of that product, publication, or service.

Copyright © 2014, INFORMS

Please scroll down for article—it is on subsequent pages



INFORMS is the largest professional society in the world for professionals in the fields of operations research, management science, and analytics.

For more information on INFORMS, its publications, membership, or meetings visit <http://www.informs.org>

# Modeling Influenza Pandemic and Planning Food Distribution

Ali Ekici

Department of Industrial Engineering, Özyeğin University, Istanbul 34794, Turkey, [ali.ekici@ozyegin.edu.tr](mailto:ali.ekici@ozyegin.edu.tr)

Pınar Keskinocak, Julie L. Swann

H. Milton Stewart School of Industrial and Systems Engineering, Georgia Institute of Technology, Atlanta, Georgia 30332  
([pinar@isye.gatech.edu](mailto:pinar@isye.gatech.edu), [julie.swann@isye.gatech.edu](mailto:julie.swann@isye.gatech.edu))

Based on the recent incidents of H5N1, H1N1, and influenza pandemics in history (1918, 1957, and 1968) experts believe that a future influenza pandemic is inevitable and likely imminent. Although the severity of influenza pandemics vary, evidence suggests that an efficient and rapid response is crucial for mitigating morbidity, mortality, and costs to society. Hence, preparing for a potential influenza pandemic is a high priority of governments at all levels (local, state, federal), nongovernmental organizations (NGOs), and companies. In a severe pandemic, when a large number of people are ill, infected persons and their families may have difficulty purchasing and preparing meals. Various government agencies and NGOs plan to provide meals to these households. In this paper, in collaboration with the American Red Cross, we study food distribution planning during an influenza pandemic. We develop a disease spread model to estimate the spread pattern of the disease geographically and over time, combine it with a facility location and resource allocation network model for food distribution, and develop heuristics to find near-optimal solutions for large instances. We run our combined disease spread and facility location model for the state of Georgia and present the estimated number of infections and the number of meals needed in each census tract for a one-year period along with a design of the supply chain network. Moreover, we investigate the impact of voluntary quarantine on the food demand and the food distribution network and show that its effects on food distribution can be significant. Our results could help decision makers prepare for a pandemic, including how to allocate limited resources and respond dynamically.

**Key words:** influenza pandemic; food distribution planning; disease spread models; multiperiod facility location; dynamic update

**History:** Received: June 16, 2009; accepted: June 18, 2013. Published online in *Articles in Advance* October 31, 2013.

## 1. Introduction

Many experts believe that it is a matter of time until the next influenza pandemic occurs given the history of influenza pandemics, H5N1 outbreaks since 2003, and the H1N1 pandemic of 2009 (Harmon 2011). Fortunately, the previous wave of H1N1 did not cause a severe pandemic, but the continuous mutation of the virus (Centers for Disease Control and Prevention 2012), as seen in Asian flu and Hong Kong flu (Viboud et al. 2005), poses a serious threat.

Epidemiologists warn that the next influenza pandemic could infect a large portion of the world population and kill millions. The World Health Organization (WHO) estimates that 2 to 7.4 million people might die worldwide (World Health Organization 2012). Furthermore, the World Bank estimates that a severe influenza pandemic could cost the world economy more than \$3 trillion (Gale 2008).

Increased travel volumes favor the spread of infectious diseases (Lam et al. 2011), which makes surveillance and planning activities more important.

As a preparedness plan, the WHO strengthened its influenza surveillance and control systems, and it is operating more than 120 national influenza centers in over 90 countries (World Health Organization 2012). Unlike previous influenza pandemics, the recent H5N1 outbreak gave a clear warning and has been eliminated by the monitoring and intervention efforts of the WHO (World Health Organization 2005). Recently, the outbreak of H1N1 forced the WHO to increase the alert level to phase 6 (on its six-point scale) (Chan 2009).

There have been three major cases of worldwide influenza pandemic in the 20th century, namely, Spanish flu (1918), Asian flu (1957), and Hong Kong flu (1968). There are different estimates regarding the number of deaths resulting from these three pandemics. Estimates from Smith (2006) are presented in Table 1. The most severe pandemic, Spanish flu, affected mainly people under 65 years of age, whereas the other two pandemics affected primarily infants and the elderly.

**Table 1** Influenza Pandemic Cases in History

Past pandemics	Mortality	Populations affected
1918–1919 (Spanish flu) (A/H1N1)	40 to 50 million (2.2 to 2.8%)	Persons <65 years
1957–1958 (Asian flu) (A/H2N2)	2 million (0.069%)	Infants, elderly
1968–1969 (Hong Kong flu) (A/H3N2)	1 million (0.028%)	Infants, elderly

The Department of State and the WHO support preparedness efforts in more than 75 countries (Homeland Security Council 2007). According to the WHO, all 193 member countries have some form of preparedness plans, and most industrialized countries are stockpiling antiviral drugs. Most preparation efforts focus on developing cell-culture vaccine manufacturing, stockpiling antivirals and vaccines, and plans for closing schools. However, designing response supply chains is also very important for meeting the various needs of the public during an influenza pandemic. Some of infected individuals may not be able to go to grocery stores to buy food, e.g., if they follow voluntary quarantine recommendations and stay home. The logistics of delivering basic supplies to infected or quarantined households is an important operations research question (Wu et al. 2006).

In addition to governments, many nongovernmental organizations (NGOs) have developed response plans for a potential influenza pandemic (Holmes et al. 2005, Morse et al. 2006). For example, the American Red Cross Metropolitan Atlanta Chapter (ARCMAC) has worked on determining ways to provide food (such as canned food and bread) to people who are infected and need to stay home (American Red Cross 2006). Ohio Department of Health and Ohio Food Industry Foundation (2006) prepared an influenza pandemic preparedness plan for grocery stores. Based on the lessons learned from the H1N1 experience (Trust for America's Health 2009, p. 2), "response plans must be adaptable and science-driven." Indeed, it is difficult for supply chains to respond effectively without considering the spread of the disease both geographically and over time.

In this paper, we consider the problem of providing food to people who are not able to obtain it due to illness in their household during an influenza pandemic. One of our main contributions is combining a disease spread and a network design model for planning purposes. First, we develop a disease spread model to estimate the spread of the disease geographically and over time and then construct a food distribution network based on these estimates. We consider a *capacitated multiperiod, multiechelon facility location problem* (CMF) for food distribution. We develop

algorithms to create a supply chain network that is dynamic and responsive to the changing needs of the population yet still computationally efficient so the proposed algorithms can be used operationally. The research question we are trying to answer is how to manage the uncertainty involved in food distribution planning: by developing a dynamic and responsive approach or by using excess capacity in a static approach. We also report our insights about the network (e.g., how many facilities are required and how long should they remain open?) under different scenarios. By combining epidemiological dynamics with operations research, our results shed light on how to design a responsive, multiechelon supply chain. Finally, we study the effects of voluntary quarantine on the food distribution supply chain.

The remainder of this paper is organized as follows. In §2, we present the literature on disease spread models and multiperiod facility location problems (FLPs). The disease spread model we developed and the simulation results are included in §3. Alternatives for food need estimation are presented in §4. In §5, we provide the facility location model, propose heuristic algorithms to solve it, and present the solution approaches proposed for food distribution. In §6, we provide the results of computational experiments and report the performances of the solution approaches proposed for food distribution logistics. We also provide insights about the impact of voluntary quarantine on food distribution. Finally, we conclude with future research directions regarding how to plan for an influenza pandemic.

## 2. Literature Review

There are two main streams of literature related to our research: (i) disease spread models and (ii) facility location and distribution models.

Disease spread models have been developed to predict the spread patterns and the effect of intervention strategies on populations with complex social and spatial structures. These models have been thoroughly researched for different infectious diseases such as influenza, smallpox, and severe acute respiratory syndrome (Ferguson et al. 2003, Lipsitch et al. 2003).

There are four common ways to model the spread of an infectious disease in a population: (i) differential equations (Fung et al. 2012, Hansen and Day 2011), (ii) simulation (agent-based) modeling (Dimitrov et al. 2011, Lee et al. 2010, Wu et al. 2006), (iii) random graphs (Carrat et al. 2010), and (iv) difference equations (Flahault et al. 2006, Larson 2007).

In differential equation models, every individual is assumed to be in one of the disease stages, e.g., susceptible (*S*), infected (*I*), or recovered (*R*), in an *S–I–R*

model, and the cumulative number of people in each stage is used to define the instantaneous changes. In simulation models, the entire population is identified by individuals and social contact networks, e.g., households and peer groups, and the spread of the disease is predicted by discrete event simulation modeling. A comprehensive comparison of agent-based and differential equation models is provided by Rahmandad and Sterman (2008). In random graph models, random graphs are used to construct the contact network and the spread of the disease is predicted accordingly. In models that use difference equations, the entire time horizon is divided into a sequence of time intervals, and the spread of the disease is predicted iteratively. The spread in each time interval is defined as a function of the spread in the previous intervals. Difference and differential equation models are both compartmental models (Jacquez 1972) and are essentially equivalent when the time intervals are very small. Another feature that distinguishes disease spread models is the mixing assumption. The chance of an individual getting infected is the same for each individual in homogeneous mixing, whereas in heterogeneous mixing the chance of infection depends on the number of contacts the person makes during the day, which varies from person to person. Thus, disease spread models with a heterogeneous mixing assumption are more accurate depictions of real-life settings, but as expected they are more complex than models based on homogeneous mixing. A summary of the literature on modeling pandemic influenza and annual influenza is provided in the online supplement (available at <http://dx.doi.org/10.1287/msom.2013.0460>).

Two performance measures, namely, *peak prevalence* and *infection attack rate* (IAR) (Rahmandad and Sterman 2008), are commonly used to evaluate the effectiveness of intervention policies. Peak prevalence is the maximum percentage of the population that is infected (symptomatic or hospitalized) at a given time, which is also related to the maximum capacity for the resources that governments and NGOs may need to serve the needs of the public. On the other hand, IAR is the cumulative percentage of people who have been exposed to the virus during the course of the disease, and it is related to the total amount of resources required during the course of the disease. School or workplace closures and other social distancing measures, such as travel restrictions and quarantine, can reduce the peak prevalence but may not significantly affect IAR (Ferguson et al. 2005, Germann et al. 2006, World Health Organization 2005). For example, social distancing measures only delayed the spread of the 1918 and 1957 pandemics (World Health Organization 2005, World Health Organization Writing Group 2006), but had little

impact on IAR. Nevertheless, delaying the spread and peak is desirable for planning purposes because it provides more time for preparedness efforts, and a flattened spread (with a smaller peak) decreases the probability of interruption of services and is less likely to result in capacity bottlenecks in response activities.

To determine the location of the food distribution facilities and their opening and closing decisions, we need to know the geographical spread of the disease. The spread pattern and the pace of the disease significantly affect the number of infected people and, thus, the demand for food. In addition, interventions can affect age groups differently. Thus, we develop a simulation-based disease spread model with *heterogeneous* mixing to predict the spread pattern of the disease and demand for food both *geographically* and *temporally*.

Given the spatial and temporal estimates of the spread of the disease and demand for food, our goal is to determine the location of food distribution facilities and when to open and close them. This is a capacitated multiperiod, multiechelon facility location problem. A thorough discussion of multiechelon FLPs can be found in the studies by Geoffrion and Graves (1974) and Hindi and Basta (1994).

Capacitated and uncapacitated multiperiod FLPs have been studied in the literature (Shulman 1991, Van Roy and Erlenkotter 1982), and various solution approaches have been proposed (Erlenkotter 1981). A popular solution approach for multiperiod FLP is to generate alternative solutions for the single-period problem and determine the best combination of these solutions using dynamic programming (Ballou 1968, Sweeney and Tatham 1976).

Multiperiod FLPs in multiechelon settings have also been studied by several authors. For example, Canel et al. (2001) and Hormozi and Khumawala (1996) study multiperiod two-echelon FLPs assuming that the facilities in the first echelon are fixed and consider opening and closing decisions for the second set of facilities only. Hinojosa et al. (2000) also consider a capacitated multicommodity, multiperiod, multiechelon FLP and propose a Lagrangean relaxation scheme with a heuristic algorithm for finding feasible solutions. Unlike Canel et al. (2001) and Hormozi and Khumawala (1996), they consider opening and closing decisions for the facilities in both echelons. Starting with a set of open facilities at the beginning of the planning horizon, they consider only the closing of currently open facilities and the opening of currently closed facilities.

The main differences between CMF and other multiperiod, multiechelon FLPs in the literature are (i) the two levels of facilities for which opening and closing decisions have to be made during the planning horizon and (ii) the flexibility of making multiple opening and closing decisions for facilities at any time



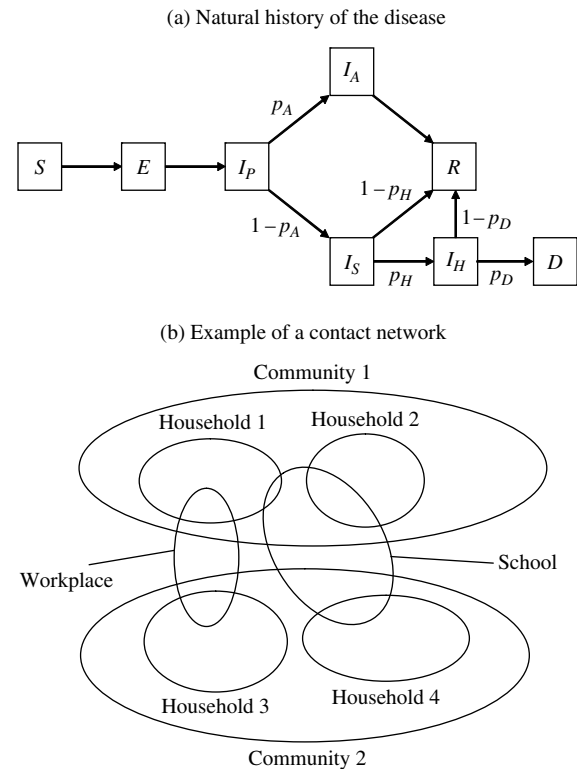
during the planning horizon rather than making one-time only opening and closing decisions for currently closed and open facilities, respectively. Because real-world examples of CMF are large (even single-period instances can be hard to solve optimally), we develop heuristic algorithms to solve CMF efficiently. Moreover, our solution approach links the disease spread model and the facility location model and allows for dynamic disease spread updates as the epidemic unfolds.

### 3. Disease Spread Model, Results, and Validation

We construct an agent-based continuous-time stochastic model for influenza transmission. We start with the model developed by Wu et al. (2006) as the basis and extend it as follows. First, we divide the entire population into different age groups, which helps model the various types of interactions between people in the population. Then, we divide the day into two time intervals corresponding to night and day to account for household and peer group interactions separately. Finally, we construct the base model for each community (census tract in our case) and connect these communities to each other by using schools and workflow data to develop a model that has a spatial component. Next, we extend the base model to investigate the effects of voluntary quarantine on the spread of disease. Voluntary quarantine is defined as encouraging a household to stay home while one or more of the household members are sick. Because it is voluntary, individuals comply with a certain probability. Below we provide a summary of the disease spread model. Additional details and a discussion of voluntary quarantine are provided in the online supplement.

The disease spread model is composed of two parts: (i) the progress of the disease for an infected individual and (ii) the spread of the disease between the members of the population (see Figure 1). An infected individual goes through the stages of the disease according to the natural history of the influenza pandemic, as described by Wu et al. (2006) (see Figure 1(a)). The progress of the disease depends on the age of the individual (Wallinga et al. 2006). Hence, we divide the population into five age groups: 0 to 5, 6 to 11, 12 to 18, 19 to 64, and 65+. Each individual is assumed to be in one of the following stages at a given time: susceptible ( $S$ ), exposed ( $E$ ), presymptomatic ( $I_P$ ), asymptomatic ( $I_A$ ), symptomatic ( $I_S$ ), hospitalized ( $I_H$ ), recovered ( $R$ ), or dead ( $D$ ). In Figure 1(a),  $p_A$ ,  $p_H$ , and  $p_D$  represent the probabilities of not developing symptoms, hospitalization for a symptomatic individual, and death for a hospitalized individual, respectively. We summarize the values of the parameters for the natural history of the

Figure 1 Two Main Components of the Disease Spread Model



disease and the relevant references in Table OS-2 of the online supplement.

We model the spread of the disease between the members of the population via a contact network (see Figure 1(b)). Given the importance of age, population density, and geography for predicting the spread of disease (Grais et al. 2003), we construct a model that takes into account population heterogeneities. For example, children are considered to play a major role in the transmission of influenza (Viboud et al. 2004) because they are assumed to be more susceptible due to lower immunity and to have more daily contacts through schools and play groups than adults have in workplaces.

First, the entire population is divided into communities that correspond to neighborhoods. The communities are linked to each other via peer groups, which account for the intercommunity spread of the disease and may be determined by age. In our model, we consider three levels of mixing: (i) community (day and night), (ii) peer group (day), and (iii) household (night) (see Figure 1(b)). All of the individuals mix in the community during the day via visits to common areas such as grocery stores, churches, etc. The children in the first three age groups (0 to 5, 6 to 11, and 12 to 18) mix with other children in kindergarten and elementary and secondary schools. People in the age group 19 to 64 are considered working adults, and they mix in workplaces with other adults. In the

base model, we assume that 50% of adults and 100% of children do not mix in their peer groups when symptomatic (Wu et al. 2006). In the case of H1N1, the Centers for Disease Control and Prevention suggested that children with flu-like symptoms should stay home, which is also consistent with our assumption (Robelen 2009). The elderly are assumed to mix in the community only (Ferguson et al. 2005, Germann et al. 2006). In retirement communities, elderly persons mix only during social times such as mealtimes (Culler and Keller 2010), which is a much more limited interaction than in schools or crowded office buildings. A susceptible individual may thus acquire an infection from other individuals in her or his household, peer group, or the community with different probabilities (contact rates). We assume a constant import rate (1.5 infected individuals per day per 100,000 people) for each community, which represents the number of infected people coming from outside the contact network (Wu et al. 2006).

A comparison of the most relevant models in the influenza pandemic literature and our disease spread model is provided in Table OS-3 of the online supplement. To summarize, we develop a detailed *SEIR* (susceptible-exposed-infected-recovered) disease spread model with a spatial (geographical) component, age-based structure, heterogeneous mixing, and night/day differentiation.

Our disease spread model is generic and can be applied to any geographical area. Given our collaborations with the ARC-MAC, the Georgia Department of Education, and the Georgia Department of Community Health, we construct our disease spread model for the entire state of Georgia. There are 159 counties and 1,615 census tracts in the state of Georgia, with a total population around 9 million (U.S. Census Bureau 2000). We consider each census tract as a single community to form the households and peer groups and to identify the sizes of the age groups. A census tract is a small subdivision of a county that generally has a population between 1,500 and 8,000 (U.S. Census Bureau 2000).

An important parameter in the model is the basic reproductive number ( $R_0$ ), which is the average number of secondary cases caused by an infectious individual (Heesterbeek 2002) and determines the infectivity of the virus. For example, the  $R_0$  value for the Spanish flu in 1918 is estimated to be in the range [1.7, 2.0] (Ferguson et al. 2006) or [2, 3] (Mills et al. 2004). On the other hand, the  $R_0$  value for the 1957 pandemic is estimated to be in the range [1.5, 1.7] (Ferguson et al. 2006), whereas the  $R_0$  value for the 1968 pandemic is estimated to be 1.89 (Rvachev and Longini 1985).

We ran simulations for a range of  $R_0$  values to account for low ( $R_0 = 1.5$ ), medium ( $R_0 = 1.8$ ), and

**Figure 2** Daily Incidence of Infection Under No Intervention

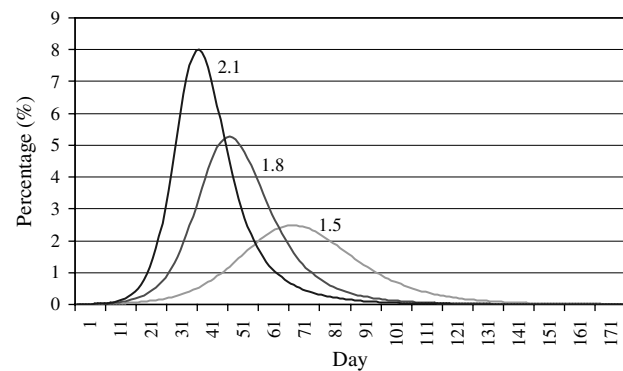


**Table 2** Results of the Disease Spread Model Under No Intervention

$R_0$	Peak prevalence (%)	Peak day	CAR (%)	IAR (%)	Mortality rate (%)
1.5	2.48	70	32.50	49.65	0.57
1.8	5.27	50	44.20	67.49	0.80
2.1	8.01	40	51.27	78.27	0.93

high ( $R_0 = 2.1$ ) infectivity. Figure 2 shows the daily incidence of infection among the population of Georgia for different  $R_0$  values. Table 2 summarizes the simulation results as an average of 20 runs in the absence of intervention policies. Peak prevalence and IAR are defined in §2. *Peak day* is the time when the percentage of the infected population is at its maximum. *Clinical attack rate* (CAR) is the cumulative percentage of people who have been symptomatic, and *mortality rate* is the percentage of the people who have died because of influenza during the course of the pandemic.

As discussed previously, the parameters of our disease spread model are in line with the literature. To further validate our model, we calibrated the model parameters to obtain the age-specific clinical attack rates of the 1957 influenza pandemic reported by Chin et al. (1960) (see §5 of the online supplement for details). We obtained similar age-specific clinical attack rates for an  $R_0$  value of 1.58, which is also consistent with the estimated  $R_0$  value of 1.5 to 1.7 for the 1957 pandemic (Ferguson et al. 2006). Similar calibration procedures have been used by others (Ferguson et al. 2005, Longini et al. 2005, Patel et al. 2005).

## 4. Estimating the Need for Food

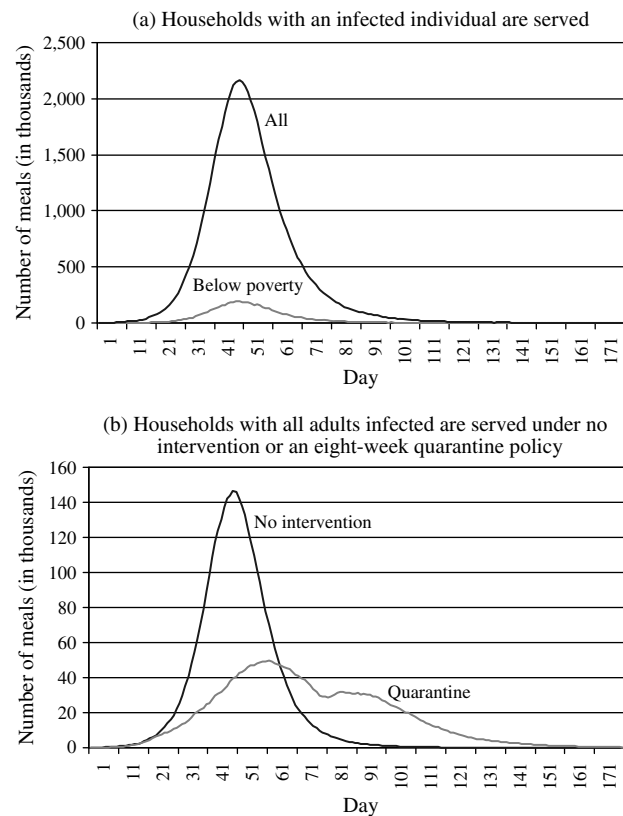
In this section, we propose several alternatives for estimating the need for food in an influenza pandemic. In the state of Georgia, the ARC-MAC has taken on the responsibility of feeding people in the case of an influenza pandemic, and our research is motivated by their planning process. Although the ARC-MAC focuses primarily on the metropolitan

Atlanta area, it also leads discussions with other organizations on planning food distribution at the state level.

In the remainder of this paper, we assume  $R_0 = 1.8$  and design a food distribution supply chain network for use during an influenza pandemic. We first determine the number of individuals who are in need of food in a census tract on a given day using the outcome of the disease spread model and multiply this number by three (assuming that an individual needs three meals per day) to calculate the total number of meals needed in this census tract on this day. There are several alternatives for calculating the need for food depending on who needs to be fed: (i) serve households with at least one infected (symptomatic or hospitalized) individual (Figure 3(a)), (ii) serve households with at least one infected individual that are below the poverty line (Figure 3(a)), (iii) serve households with all adults infected (Figure 3(b), under no intervention and eight-week quarantine starting at the fourth week), (iv) serve households with all adults infected that are below poverty line, and (v) serve the households under voluntary quarantine, i.e., if an individual from that household develops symptoms or is hospitalized (in either case, all members of this household are advised to stay home, and they choose to stay home with a certain probability, 50% in our case). If the members of a household are advised to stay home due to an infection in the household, this household is called “quarantined.” Once a household is quarantined, if no other individual in the household develops symptoms or is hospitalized within a week, the quarantine is released. Otherwise, quarantine is extended for another week for that household. Because of the negative effects of prolonged quarantine, we consider a limited-time voluntary quarantine. For example, an eight-week voluntary quarantine is imposed (or encouraged) for a duration of eight weeks by public health officials (although the quarantine duration for a given household is often much shorter, e.g., one to three weeks, depending on the number of individuals in the household and when they get sick), and then it is released entirely.

In Figure 3(a), the number of meals required is high compared with other options because all of the households with an infected individual are served in this case. In Figure 3(b), we observe two peaks during an eight-week quarantine. After the quarantine is released, the second (lower) peak occurs due to the increased number of interactions in the community. In the remainder of this paper, we consider the case of serving households with all adults infected, but the approach is valid for alternative ways of calculating the need for food.

**Figure 3** Number of Meals Needed Daily for Different Alternatives



## 5. Facility Location Model and Solution Approaches for Food Distribution

In this section, we explain CMF and propose a mixed integer linear formulation. CMF is NP-hard, and large instances cannot be handled using commercial solvers such as CPLEX. Hence, inspired by the add (Kuehn and Hamburger 1963) and drop (Cooper 1964) heuristics proposed for FLPs, we propose a heuristic algorithm called *single-period add-drop heuristic* (SPAD). An example of an add-drop heuristic can be found in the study by Narula and Ogbu (1979) in the context of determining the location of health-care centers and hospitals. We develop new aspects to capture the multi-echelon structure of the problem and the demand dynamics of a multiperiod setting. Furthermore, we propose two solution approaches (static and dynamic) for planning food distribution during an influenza pandemic.

We model three echelons in the distribution network: supply points (SPs), major facilities (MFs; where the food is processed and/or packed for easy pick-up by individuals), and points of delivery (PODs; e.g., schools, churches, community centers, and businesses). Individuals and households who are in need are able to obtain food from the PODs

**Table 3** Notation Used in the Formulation

$T$	Length of the planning horizon (in weeks)
$N_1, N_2, N_3, N_4$	Sets of supply points, major facilities, PODs, and demand nodes, respectively
$S_i$	Number of meals that can be supplied by supply point $i$ for $i \in N_1$
$F_j$	Fixed cost incurred if facility $j$ is open during a week for $j \in N_2 \cup N_3$
$f_j, g_j$	Cost of opening and closing facility $j$ for $j \in N_2 \cup N_3$
$c_o^1, c_o^2$	Unit material (meal) handling cost at a major facility and POD, respectively
$C_j$	Capacity (in terms of number of meals) of facility $j$ for $j \in N_2 \cup N_3$
$D_{kt}$	Number of meals needed at demand node $k$ in week $t$ for $k \in N_4, t \in \{1, \dots, T\}$
$d_{ij}$	Distance (in miles) between node $i$ and node $j$ for $i \in N_k, j \in N_{k+1}, k \in \{1, 2, 3\}$
$c_u^1$	Unit transportation cost of a meal from a supply point to a major facility per mile
$c_u^2$	Unit transportation cost of a meal from a major facility to a POD per mile
$c_u^3$	Unit transportation cost of a meal from a POD to a demand node per mile

(which we assume can be run with minimum personal contact; e.g., individuals could drive through and someone puts the food into the trunk of their car). Other ways of distribution can be determined for those without transportation. In our food distribution network, each census tract is considered a demand node (DN), and the level of demand is determined by the number of individuals in need. We assume that the locations of major facilities and PODs are already known, and decisions need to be made about (i) where and when to open and close them and (ii) how to allocate the food among the major facilities and the PODs with the goal of minimizing the total cost of serving the target population, given the estimates of demand across area and time. We consider closing and opening decisions on a weekly basis.

### 5.1. Mixed Integer Linear Model

We develop a mixed integer linear formulation for CMF (Table 3 summarizes the notation) assuming that the demand, i.e., the number of meals needed each week in the planning horizon for each census tract, is known. We obtain demand estimates (which are then input to the CMF formulation) by running the disease spread model. Note that any other model that estimates the demand for food geographically and temporally can also be used to generate the input for CMF.

The objective of our model is to minimize the total cost (including the travel cost incurred by individuals picking up their food) while satisfying demand. Note that if we ignore the individuals' travel costs (or an explicit upper bound on the travel distance in the constraints), the model will locate all the major facilities and PODs close to the supply points, which is not acceptable in a disaster relief or emergency response

setting due to high societal costs. The variables used in the formulation are as follows:

$x_{ijt}$  = number of meals sent from node  $i$  to node  $j$  in week  $t$   $i \in N_k, j \in N_{k+1}, k \in \{1, 2, 3\}, t \in \{1, \dots, T\};$

$y_{jt} = \begin{cases} 1 & \text{if facility } j \text{ is open during week } t, \\ 0 & \text{otherwise,} \end{cases} \quad j \in N_2 \cup N_3, t \in \{1, \dots, T\};$

$w_{jt} = \begin{cases} 1 & \text{if facility } j \text{ is opened at the beginning of week } t, \\ 0 & \text{otherwise,} \end{cases} \quad j \in N_2 \cup N_3, t \in \{1, \dots, T\};$

$z_{jt} = \begin{cases} 1 & \text{if facility } j \text{ is closed at the end of week } t, \\ 0 & \text{otherwise,} \end{cases} \quad j \in N_2 \cup N_3, t \in \{1, \dots, T\}.$

Using these variables, the objective function can be written as

$$\begin{aligned} \mathcal{CF}(x, y, w, z) = & \sum_{t=1}^T \sum_{i \in N_1} \sum_{j \in N_2} (d_{ij} c_u^1 x_{ijt} + c_o^1 x_{ijt}) \\ & + \sum_{t=1}^T \sum_{i \in N_2} \sum_{j \in N_3} (d_{ij} c_u^2 x_{ijt} + c_o^2 x_{ijt}) \\ & + \sum_{t=1}^T \sum_{j \in N_3} \sum_{k \in N_4} d_{jk} c_u^3 x_{jkt} \\ & + \sum_{t=1}^T \sum_{j \in N_2 \cup N_3} (F_j y_{jt} + f_j w_{jt} + g_j z_{jt}). \end{aligned}$$

The mathematical formulation of CMF is as follows:

$$\text{minimize } \mathcal{CF}(x, y, w, z) \quad (1)$$

$$\text{s.t. } \sum_{j \in N_2} x_{ijt} \leq S_i \quad i \in N_1, t \in \{1, \dots, T\}; \quad (2)$$

$$\sum_{j \in N_3} x_{jkt} \geq D_{kt} \quad k \in N_4, t \in \{1, \dots, T\}; \quad (3)$$

$$\sum_{i \in N_k} x_{ijt} \leq C_j y_{jt} \quad j \in N_{k+1}, k \in \{1, 2\}, t \in \{1, \dots, T\}; \quad (4)$$

$$\sum_{i \in N_k} x_{ijt} = \sum_{l \in N_{k+2}} x_{jlt} \quad j \in N_{k+1}, k \in \{1, 2\}, t \in \{1, \dots, T\}; \quad (5)$$

$$w_{jt} \geq y_{jt} - y_{j,t-1} \quad j \in N_2 \cup N_3, t \in \{1, \dots, T\}; \quad (6)$$

$$z_{jt} \geq y_{jt} - y_{j,t+1} \quad j \in N_2 \cup N_3, t \in \{1, \dots, T\}; \quad (7)$$



$$y_{j0} = 0 \quad j \in N_2 \cup N_3; \quad (8)$$

$$y_{jT+1} = 0 \quad j \in N_2 \cup N_3; \quad (9)$$

$$y_{jt} \in \{0, 1\} \quad j \in N_2 \cup N_3, \quad t \in \{1, \dots, T\}; \quad (10)$$

$$w_{jt} \geq 0 \quad j \in N_2 \cup N_3, \quad t \in \{1, \dots, T\}; \quad (11)$$

$$z_{jt} \geq 0 \quad j \in N_2 \cup N_3, \quad t \in \{1, \dots, T\}; \quad (12)$$

$$x_{ijt} \geq 0 \quad i \in N_k, \quad j \in N_{k+1}, \quad k \in \{1, 2, 3\}, \\ t \in \{1, \dots, T\}. \quad (13)$$

In the above model, the objective function (1) represents the summation of handling costs, facility operating costs, facility opening and closing costs, and total transportation costs including individuals' travel costs. Constraints (2) and (3) are the supply and demand constraints, respectively. Capacity constraints for each facility (either a major facility or a POD) and flow balance constraints are represented by constraints (4) and (5), respectively. Constraints (6) and (7) restrict service to open facilities. Constraints (8) and (9) set the initial and final values. Finally, constraints (10)–(13) are the integrality and sign restrictions. Note that the nonnegativity constraints for  $w_{jt}$  and  $z_{jt}$ , the objective function, and the binary structure of  $y_{jt}$  ensure that  $w_{jt}$  and  $z_{jt}$  are 0 or 1.

Commercial optimization software such as CPLEX 12.4 can handle medium-sized instances (with up to 167 demand nodes, 72 PODs, 10 major facilities, and 20 supply points in our experiments) for medium and high shipment cost settings. The performance of CPLEX is worse on instances with low shipment cost. To find near-optimal solutions for large instances, we propose heuristic approaches, which are explained in §5.2.

## 5.2. Heuristics for CMF

In this section, we explain SPAD and its variants, namely, the *single-period optimal heuristic* (SPO) and *single-period hybrid heuristic* (SPH). The pseudocode for SPAD is provided in §7 of the online supplement. In both SPAD and its variants, for each period we solve two single-period FLPs to determine which PODs and major facilities to open; that is, for period  $t$ , first we solve a single-period version of CMF assuming that the demand of node  $k$  is a weighted average of future demands (with weights decreasing over time) as follows:

$$\bar{D}_{k,t+1} = \sum_{j=t+1}^{T-1} \frac{D_{kj}}{2^{j-t}} + \frac{D_{kT}}{2^{T-1-t}}. \quad (14)$$

The solution to this problem helps us predict the major facilities and PODs that could eventually be opened. Then, considering the estimated future decisions and the decisions made in the previous period,

we solve a single-period FLP with the demand of node  $k$  as  $D_{kt}$  to determine which major facilities and PODs to open in period  $t$ .

SPAD, SPO, and SPH differ in terms of the methods they use for solving the two single-period FLPs. In SPAD, we use the “add-drop subroutine.” In the “add” part, the demand nodes are assigned to the nearest POD while taking into account the capacities of the PODs. Then, in the “drop” part considering the savings achieved by closing a POD and assigning its demand to other nearby PODs, we close PODs one at a time as long as there is a positive saving. Next, assuming that the remaining open PODs represent the demand nodes, we apply similar steps to determine which major facilities to open.

In SPO, we solve both of the two single-period FLPs optimally. SPO requires longer run times, but may find a solution with a lower cost. In SPH, we combine SPAD and SPO such that in each period we solve the first problem with the (weighted) average of the future demand using the add-drop subroutine and solve the second problem with the current period's demand optimally. In addition to SPAD, SPO, and SPH, we consider a greedy algorithm, called the *myopic heuristic* (MH), where the single-period problem is solved (using the add-drop subroutine) in each period without considering future decisions. We test SPAD, SPO, SPH, and MH on a set of instances and compare the solution times and the optimality gap of the solutions found by them in §6.

## 5.3. Solution Approaches for Planning Food Distribution

In this section, we discuss solution approaches for food distribution logistics planning during an influenza pandemic. At the beginning of the planning horizon, the up-to-date spread of the disease (the number of people in each disease stage in each census tract) is used as an input (initial conditions) to the disease spread model. The average of multiple simulation runs is used to estimate the number of people in each disease stage (and the total size of the households with all adults infected) in each census tract on each day of the entire planning horizon. Then, we estimate the food demand for each period of the entire planning horizon, assuming we feed the households with all adults infected (see §4, alternative (iii)). The estimated food demand is input to the CMF, which is solved by the heuristics proposed in §5.2, to make the opening, closing, and resource allocation decisions. We propose two approaches for planning food distribution:

- *Static approach* (STAT). In STAT, the decisions about when and where to open and close facilities are made once at the beginning for the entire planning horizon.

The advantage of STAT is its simplicity of implementation. However, as the disease progresses and more information becomes available regarding the spread of the disease over time, it is possible to dynamically update and improve the decisions, which motivates the second approach:

- *Dynamic update approach* (DYN). In DYN, we implement the decisions only for the first few, say,  $\tau$ , periods (weeks in our case). After  $\tau$  periods, the up-to-date spread of the disease is input to the disease spread model, and the average of multiple simulation runs is used to estimate the spread of the disease (and the corresponding food demand) for the remainder of the planning horizon. The updated demand estimates are then fed into CMF to obtain facility location and resource allocation decisions for the remainder of the planning horizon. The ending conditions (open and closed facilities) at the end of  $\tau$  periods are used as the initial conditions of the following period. This folding horizon approach decreases the deviation of the estimates from the real-world situation.

In both DYN and STAT, in each period after the facility opening and closing decisions are made, the realized demand is satisfied as capacity permits. Shipment decisions are made based on the realized demand by solving a single-period version of CMF with facility opening and closing decisions fixed, and the excess demand remains unsatisfied.

## 6. Computational Results

In this section, we provide the results of the computational experiments. First, we test the performances of the proposed heuristics to solve CMF. Then, we compare the performances of STAT and DYN against each other and against other simple policies proposed by the ARC-MAC. Finally, we present our analysis of the impact of voluntary quarantine on food distribution.

### 6.1. Test Instances

To evaluate the performances of the heuristics, we consider Gwinnett county, Fulton county, and the metropolitan Atlanta area (containing 71, 167, and 603 census tracts, respectively) as test cases. We assume that we serve food to people when more than 0.5% of the population is infected at a given time, corresponding to an eight-week time interval (between weeks 5 and 12) when  $R_0 = 1.8$ . Although the exact percentage is hard to estimate, this assumption is reasonable because NGOs and/or governments will not construct a large food distribution network if the number of infections is under some threshold value. For example, Germann et al. (2006) consider initiating the intervention strategies 7 (or 14) days after issuing a pandemic alert, and they assume that a pandemic alert is triggered when the total number of symptomatic individuals reaches 10,000. Hence,

the length of the planning horizon is eight (weeks) in the test instances.

Based on the estimations provided by the ARC-MAC, the capacity of a typical POD is assumed to be around 10,000 meals per week. Hence, the capacity of each POD is uniformly generated from the interval  $[8,000, 12,000]$ . The total capacities of the major facilities and supply points are equal to the total capacity of the PODs. Depending on the number of major facilities and supply points in each instance (see Table 4), the total capacity is distributed evenly among the major facilities and supply points. The ARC-MAC is planning to use places such as schools and churches as PODs and make agreements with grocery stores and charity foundations to use them as supply points. Potential POD locations are available in almost every neighborhood, but the locations of supply points are not yet finalized; hence, we randomly assigned POD locations and supply points to the census tracts in the computational experiments. For the metropolitan Atlanta area instances, based on the discussions with the ARC-MAC, we assigned the major facility locations to the most crowded census tracts of the 10 most densely populated counties (Carroll, Cherokee, Clayton, Cobb, DeKalb, Douglas, Fayette, Fulton, Gwinnett, and Henry), with at most one major facility per county (see the map in §8 of the online supplement for the counties located in the metropolitan Atlanta area). This is mainly because densely populated areas are expected to be affected heavily by the influenza pandemic, and demand is going to be larger in these areas. For small (Gwinnett county) and medium (Fulton county) instances, we randomly assigned the locations of the major facilities to the census tracts. The opening, closing, and fixed operating costs of the PODs and major facilities are proportional to the square root of the capacity of the relevant facility since facility-related costs are often represented by a concave function of capacity due to economies of scale (Feldman et al. 1966). The opening, operating, and closing costs of a major facility are 10 times that of a POD of the same size since most of the food processing and/or packing operations will be performed in major facilities. The opening cost is assumed to be two times the closing cost and four times the fixed operating cost. The shipments from the supply points to the major facilities and from the major facilities to the PODs will be large and performed by trucks. However, for shipments from PODs to households, either an individual from the household will drive to a POD, or a small truck will distribute to households. Because of this, the unit shipment costs from supply points to major facilities ( $c_u^1$ ) and from major facilities to PODs ( $c_u^2$ ) are assumed to be equal to each other and to 50% of the unit shipment cost from PODs to demand nodes ( $c_u^3$ ).

The distances between the facility locations and census tracts are calculated as Euclidean distances using the longitude and latitude of the centroids of the census tracts. Finally, we consider three different settings for shipment costs, namely, low, medium, and high. In the “low” setting the facility-related costs dominate the objective function, in the “medium” setting the shipment costs and facility-related costs are comparable, and in the “high” setting the shipment costs dominate.

## 6.2. Performances of the Heuristics

We compared the average performances of the heuristics for each of the three shipment cost settings (low, medium, high). We used CPLEX 12.4 as the optimization engine and imposed an optimality gap of 0.01% as the stopping criterion, i.e., it will terminate if the upper and lower bounds are within 0.01%. All computational experiments are carried out on Intel Xeon 2.27 GHz dual core Linux servers with 4 GB random access memory. For finding the optimal solution, we set a time limit of 8 hours for the small and medium instances (Gwinnett and Fulton counties) and 12 hours for the metropolitan Atlanta area instances. We set a time limit of 0.5 hour and 1 hour for each single-period problem in SPO and SPH, respectively, since two optimization problems are solved in SPO in each period, whereas only one optimization problem is solved in SPH in each period. The detailed results (central processing unit (CPU) times and optimality gaps with respect to the best lower bound) are presented in Table 4. The optimality gaps are calculated as the percentage difference between the heuristic solution and the optimal solution or the best lower bound found by CPLEX. For each parameter setting, we generated 20 different instances, and the results presented are the average of these 20 instances. The optimality gaps are conservative estimates since they are calculated with respect to the best lower bound found by CPLEX within the time limits.

From Table 4, we see that if the shipment costs dominate the objective function, CMF is “easy” to solve (i.e., we can find an optimal solution using CPLEX in less than three minutes for small and medium instances, and the optimality gap of the solutions found at the end of the time limit is less than 0.1%, on average, for large instances) because almost all of the facilities are open during the entire planning horizon. One simply assigns each demand point to the closest facility.

As the instances become larger, we observe that the best integer solution found by CPLEX at the end of the time limit is significantly worse than the solutions found by the heuristics. Even if we increase the time limit, CPLEX cannot handle large instances since the computer runs out of memory.

The solutions found by SPO and SPH are very close to each other, and the average optimality gap is around 2.5%. However, the solution time of SPH is around 30% that of SPO. The solution times required for SPAD and MH are negligible compared to SPO and SPH, but the average optimality gaps are around 3.9% and 5.5%, respectively. Hence, we propose using SPH and SPAD to solve CMF. Furthermore, for very large instances, such as the entire state of Georgia, SPAD is the best alternative since in this case even a single-period problem is difficult to handle using commercial optimization software.

Finally, we conduct additional experiments where we increase the number of major facilities, PODs, and supply points by five in the first (71 DN, 36 POD, 5 MF, 10 SP) and second (167 DN, 36 POD, 5 MF, 10 SP) sets of instances. We summarize these results in §9 of the online supplement. Based on these experiments, we conclude that it is the number of major facilities that makes CMF difficult. These results also indicate that if the location of the major facilities can be determined or fixed independently, the corresponding CMF can be solved more easily even when dynamically considering changes in the spread of the disease.

## 6.3. Static vs. Dynamic Update Approach

In this section, we first compare the performances of STAT, DYN, and the simple policies proposed by the ARC-MAC, as well as a benchmark case, “perfect solution,” which is the solution obtained assuming that we know the real-world spread of the disease ahead of time. This is impossible to know, but provides an opportunity to evaluate the performances of our solution approaches. Since large instances cannot be solved optimally using CPLEX, we consider Gwinnett county as the test case with 5 major facilities, 36 PODs, and 10 supply points. We solve CMF optimally to compare STAT and DYN.

Let  $DYN(\tau)$  denote the implementation of DYN with a rolling horizon of  $\tau$ , i.e., demand estimates and decisions are updated every  $\tau$  periods (weeks in our case). Based on discussions with the ARC-MAC, we tested  $DYN(1)$  and  $DYN(2)$ , i.e., decisions are updated weekly or biweekly, respectively. Whereas  $DYN(1)$  may be more responsive to potential changes in demand,  $DYN(2)$  may cause less schedule nervousness.

The same setting described in §6.1 is used in these experiments. The benchmark case (real-world scenario), including the number of people in each disease stage in each census tract and the demand for food on each day, is generated by a single simulation of our disease spread model. The demand estimates in  $DYN(1)$  and STAT are calculated by taking the average of five simulation runs. We compare the



**Table 4** Experiments to Test the Performances of the Heuristics with CPU Time in Seconds and Gap Compared to the Best Lower Bound

Instance	Algorithm	Shipment cost					
		Low		Medium		High	
		CPU	Gap (%)	CPU	Gap (%)	CPU	Gap (%)
71 DN, 36 POD, 5 MF, 10 SP	MH	0.2	5.97	0.2	5.16	0.2	5.23
	SPAD	0.2	5.39	0.2	3.22	0.2	3.17
	SPO	10.0	1.44	5.5	1.84	4.3	1.87
	SPH	3.3	1.92	2.0	1.71	1.6	1.26
	Best integer solution	1,725.9	0.00	121.8	0.00	38.6	0.00
167 DN, 36 POD, 5 MF, 10 SP	MH	0.4	4.31	0.5	1.73	0.4	1.91
	SPAD	0.4	3.97	0.4	1.53	0.4	1.56
	SPO	26.4	0.94	11.8	1.03	8.0	0.82
	SPH	6.2	1.81	3.8	0.92	2.9	0.87
	Best integer solution	4,957.9	0.00	357.5	0.00	141.7	0.00
167 DN, 72 POD, 10 MF, 20 SP	MH	1.0	10.97	1.0	6.32	1.0	4.06
	SPAD	0.8	11.35	0.8	4.41	0.8	2.25
	SPO	302.9	8.10	139.2	2.91	84.8	1.40
	SPH	39.3	9.01	28.2	3.06	21.2	1.39
	Best integer solution	28,803.9	5.32	28,808.1	1.23	15,020.8	0.06
603 DN, 151 POD, 10 MF, 20 SP	MH	10.2	9.01	11.5	3.64	11.7	1.87
	SPAD	10.0	7.41	11.1	2.35	9.4	1.08
	SPO	17,250.3	5.75	7,549.4	1.55	6,814.8	0.61
	SPH	7,419.1	5.92	691.1	1.55	1,281.4	0.58
	Best integer solution	43,217.5	20.44	42,241.8	1.03	24,834.6	0.06

performances of STAT and DYN(1) against two other policies derived from the initial planning efforts of the ARC-MAC. The ARC-MAC initially planned to serve around 480,000 meals daily at the peak of the pandemic, which is based on the assumption of 15% prevalence at the peak (American Red Cross 2006, 2008). The initial plans were based on the assumption that demand is distributed across counties in proportion to population and without considering the opening and closing of facilities over time. This plan corresponds to using excess capacity (opening all major facilities and PODs) in our computational experiments. Therefore, in *Policy 1* (P1), we open all major facilities and PODs during the entire planning horizon and serve demand accordingly. In *Policy 2* (P2), we use the results of epidemiological modeling to update the demand estimate provided by the ARC-MAC. More specifically, we use the peak prevalence for  $R_0 = 1.8$  (which is around 5.27%) to adjust the initial demand estimate (480,000 meals per day). After calculating the new demand estimate, we determine the locations for opening major facilities and PODs by giving higher priority to the densely populated neighborhoods.

The results (average of 20 replications) in Table 5 compare the solution approaches in terms of total cost (as a percentage of the total cost of the benchmark case) and unsatisfied demand. We observe that the proposed approaches (STAT and DYN(1)) produce more cost-efficient policies compared to P1 and P2. As the shipment costs increase, the performances of

P1 and P2 improve, which is reasonable since operating more major facilities and PODs decreases the shipment costs in this case.

The locations of open major facilities are almost the same in both STAT and DYN(1) for the same shipment cost setting, in part due to the high operating costs. Moreover, since the same initial spread is used as an input for both models and the disease reaches densely populated areas regardless of where it starts, in most cases major facilities are located in densely populated areas. However, the number of PODs operated in the solution found by DYN(1) is approximately 5% higher than the number of open PODs in the solution found by STAT. In the “high” shipment cost setting, even small changes in the spread of the disease affect decisions about PODs when using DYN(1). A small change in the spread pattern and a small increase in the demand affect the locations and the number of

**Table 5** Comparison of the Policies Proposed by the ARC-MAC, STAT, and DYN(1)

Policy	Shipment cost					
	Low		Medium		High	
	Tot. cost (%)	Un. dem. (%)	Tot. cost (%)	Un. dem. (%)	Tot. cost (%)	Un. dem. (%)
P1	142.39	0.00	121.68	0.00	110.29	0.00
P2	112.42	0.00	108.31	0.00	109.48	0.00
STAT	100.90	0.00	101.13	0.00	100.85	0.00
DYN(1)	100.95	0.00	101.12	0.00	100.64	0.00

*Note.* Tot. cost, total cost; Un. dem., unsatisfied demand.



open PODs, respectively, due to lower operating costs and lower capacities compared to major facilities.

According to Table 5, the performance of STAT is close to that of DYN(1), since we assumed that we know the parameters of the disease at the beginning of the planning horizon. Next, we compare the performances of the proposed models under uncertainty in the values of the disease parameters. In addition to DYN(1) and STAT, we consider DYN(2) and a variant of STAT, denoted by STAT-2. In STAT-2, to address parameter uncertainty, we use a higher  $R_0$  value than estimated and perform the simulation runs accordingly to determine demand estimates. STAT-2 mimics the conservative approach of overestimating demand and building excess capacity to account for parameter uncertainty. More specifically, if estimated  $R_0$  is 1.5 (or 1.8 or 2.1) in STAT-2, we run the simulation model with an  $R_0$  value of 1.8 (or 2.1 or 2.4). To test the robustness of STAT, DYN(1), DYN(2), and STAT-2 under uncertainty in the disease parameters, we generate a benchmark case (real-world scenario) and conduct experiments assuming that the estimated values of the parameters are different from the actual values. Although the magnitude and pace of spread is mainly affected by  $R_0$ , we analyze the impact of a wide range of parameters provided in Table OS-10 of the online supplement.

While testing the robustness of DYN(1) and DYN(2), we do not change the estimates of the disease parameters. We only use information regarding the up-to-date spread of the disease to update the demand estimates using the disease spread model. This approach provides us with a conservative estimate of the benefits of DYN(1) and DYN(2) over STAT. Clearly, if we also update disease parameters, the benefit would be even higher.

We first perform a univariate sensitivity analysis where we assume that the estimated value of only one parameter is different from the actual value. The values of the parameters considered in the univariate sensitivity analysis and the detailed results are provided in Tables OS-11 and OS-12 of the online supplement. The univariate sensitivity analysis demonstrates that accurately estimating the values of disease parameters is important, especially for “low” and “medium” shipment cost settings. When the shipment costs are high compared to facility-related costs, there is often excess capacity due to opening large number of facilities to decrease shipment costs. This excess capacity buffers against the inaccurate estimates of disease parameters in most cases.

The performance of STAT deteriorates significantly especially under “low” and “medium” shipment cost settings when there is uncertainty in parameters such as the probability of developing symptoms, duration of the exposed stage, duration of the presymptomatic

stage, duration of the symptomatic stage, the proportion of infections at stages other than the symptomatic stage, the proportion of infections that occurs outside households, and  $R_0$ . The total cost can increase up to 10% and the unsatisfied demand can be as high as 9% under STAT. However, DYN(1) can easily adjust facility location and resource allocation decisions to address uncertainty in parameter values, i.e., in almost all cases, demand is satisfied almost 100% at the expense of a small increase in the total cost compared to the “perfect solution.”

We observe that STAT-2 demonstrates superior overall performance in terms of satisfying demand compared to STAT at the expense of a significant increase in total cost. Both STAT-2 and DYN(1) satisfy more than 99% of demand on average. However, in STAT-2, the total cost of managing the food distribution network is around 9%, 4%, and 2% higher than that of DYN(1) for “low,” “medium,” and “high” shipment cost settings, respectively. Finally, the overall performance of DYN(2) is close to that of DYN(1) in terms of both total cost and demand satisfaction percentage.

Looking at the performances of the proposed solution approaches under parameter uncertainty, we conclude that the most important parameters are  $R_0$  and the durations of the exposed, presymptomatic, and symptomatic stages. Overestimating the durations of the exposed and presymptomatic stages and underestimating the duration of the symptomatic stage and  $R_0$  may result in a significant amount of unsatisfied demand even for DYN(1).

To evaluate the combined effect of uncertainty in multiple parameters, we run simulations for two extreme cases, called *slow estimated spread* (SES) and *fast estimated spread* (FES), with parameters representing “slow” and “fast” estimated (compared to the actual) spread of the disease. The parameter values for the SES and FES scenarios are provided in Table OS-13 of the online supplement.

The results of the SES and FES scenarios are presented in Table 6. We observe that less than 45% and 60% of the demand is satisfied under STAT and STAT-2, respectively, when the estimated spread is much slower than the actual spread, whereas DYN(1) satisfies around 75% of the demand in the “low” shipment cost setting. We observe similar results with decreasing percentages of unsatisfied demand as the shipment costs increase. DYN(2) performs better than STAT and STAT-2, but results in up to 10% more unsatisfied demand compared to DYN(1). When the estimated spread is much faster than the actual spread, most of the demand is satisfied due to excess capacity; however, the total costs of STAT, DYN(1), DYN(2), and STAT-2 can be around 36%, 25%, 25%, and 36% higher than that of the benchmark case,

**Table 6 Robustness of STAT, DYN(1), DYN(2), and STAT-2 Under Two Extreme Cases**

Scenario	Criteria	Shipment cost											
		Low				Medium				High			
		STAT	DYN(1)	DYN(2)	STAT-2	STAT	DYN(1)	DYN(2)	STAT-2	STAT	DYN(1)	DYN(2)	STAT-2
SES	Tot. cost (%)	47.82	77.53	67.56	58.74	66.62	93.24	91.45	62.32	66.99	94.39	95.21	62.86
	Un. dem. (%)	56.62	24.80	35.63	43.20	39.48	10.17	13.69	37.11	37.11	9.74	10.16	37.11
FES	Tot. cost (%)	135.67	124.62	125.30	136.45	117.36	111.82	112.42	117.89	107.69	105.14	105.56	108.05
	Un. dem. (%)	0.00	0.00	0.00	0.00	0.00	0.00	0.00	0.00	0.00	0.00	0.00	0.00

Note. Tot. cost, total cost; Un. dem., unsatisfied demand.

respectively. This is mainly because of the large number of facilities operated in response to high estimated demand. As the shipment costs increase, the performances of the proposed solution approaches improve. Based on the analysis of SES and FES, we conclude that underestimating the pace of the spread can have severe consequences, such as a large number of people left unserved, and overestimating demand may pose challenges due to high capacity requirements and the short amount of time available to implement the food distribution plan. We observe that the average number of open major facilities is approximately twice as high, and the average number of PODs is two to three times as high (depending on the shipment cost setting), under the FES scenario compared to the SES scenario. However, from a societal perspective, satisfying the needs of the public to the maximum extent possible is important. Hence, organizations planning food distribution may benefit from intentionally but cautiously overestimating demand, by overestimating or underestimating (see §10 of the online supplement) the values of the parameters (or at least the most important parameters), so that the estimated spread may be faster than actual.

#### 6.4. Impact of Voluntary Quarantine on the Food Distribution Supply Chain

In this section, we investigate the effects of voluntary quarantine on food demand and the food distribution supply chain, both in terms of total cost and the quality of service, which is defined as the percentage of demand served from a POD within 10 miles of the demand location. Quality of service is important not only because of convenience to the public and potential shortages in gas supply, but also because if the infected individuals drive a long distance and make additional stops, infection could be introduced to other areas.

*A voluntary quarantine with (near-)optimal timing and length decreases the likelihood of capacity bottlenecks and supply chain disruptions significantly.* In case of an eight-week quarantine, more than 0.5% of the population is infected between weeks 6 and 18, and the reductions in the total food demand and IAR are

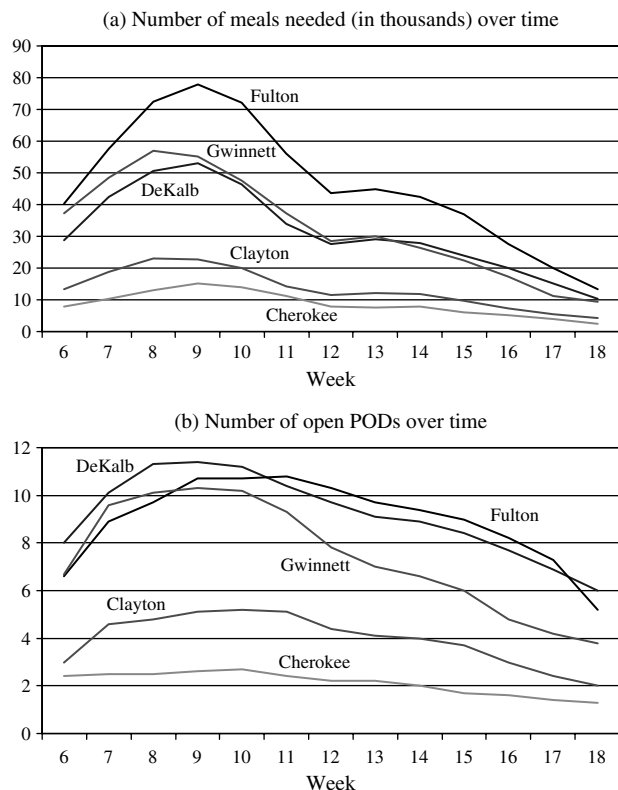
26.70% and 16.82%, respectively, when compared to the no intervention case (see §6 of the online supplement). The reduction in the average demand (over time) is even higher (55%) under voluntary quarantine since demand (and the number of infections) is more evenly spread over time (similar to Figure 3(b); see §11 of the online supplement). A similar observation is made by Rahmandad and Sterman (2008) after analyzing the effects of social distancing on the spread of the disease, and they also mention the effects of peak prevalence on the infrastructure of health services. Since the decision to quarantine is made by public health officials, our analysis of voluntary quarantine also highlights the importance and potential benefits of closer collaboration between NGOs and public health officials.

Table 7 summarizes the effects of quarantine on a large supply chain network based on the results of 10 different replications with 200 PODs, 10 major facilities, and 20 supply points in the entire metropolitan Atlanta area. The reduction in total cost under voluntary quarantine (compared to no intervention case) is higher when the shipment costs or facility-related costs dominate because the reduction in total demand is almost fully reflected in the total cost in these settings.

As shown in the third and fourth columns of Table 7, the quality of service decreases as the shipment costs decrease. This occurs because lower shipment costs increase the amount of demand served from a long distance. Additionally, we find that quality of service is better under the no intervention case

**Table 7 Comparison of Eight-Week Quarantine with No Intervention Case**

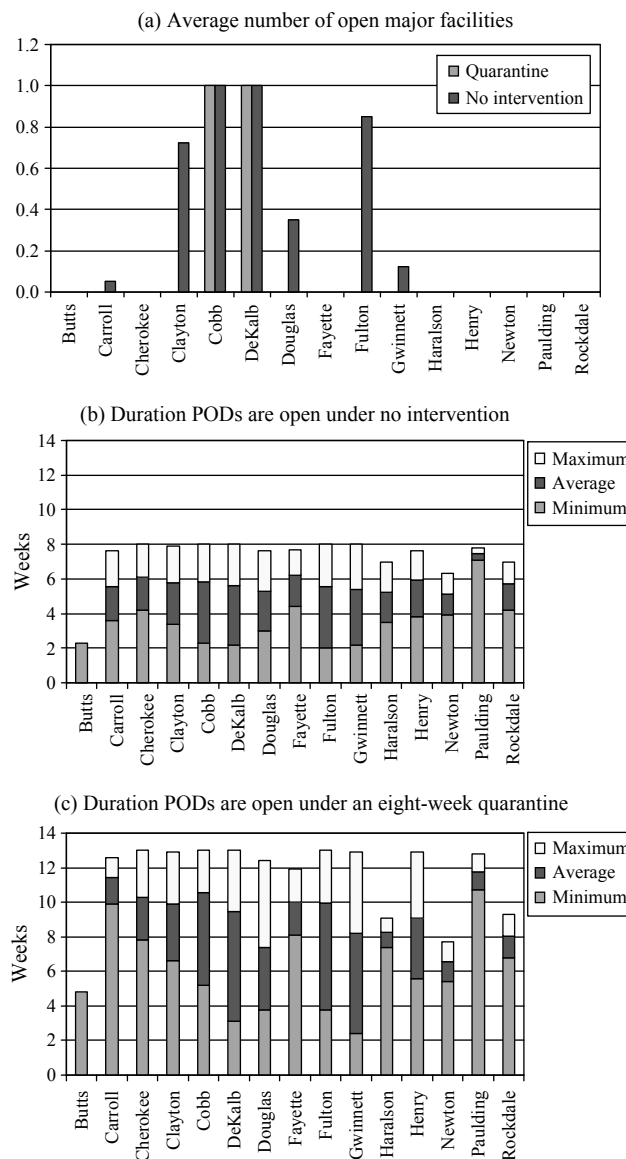
Shipment cost	Cost reduction in an eight-week quarantine compared to no intervention (%)	Demand served within 10 miles (%)	
		Eight-week quarantine	No intervention
High	22.35	99.79	99.85
Medium	18.74	97.86	99.66
Low	25.97	85.29	94.99

**Figure 4** Number of Meals and Open PODs Over Time Under an Eight-Week Quarantine

than under quarantine (if all facilities can indeed operate at the estimated capacities). Since the average demand is lower under quarantine, fewer facilities need to be operated in a given period, and this decreases the demand served within 10 miles.

We provide a detailed analysis of the “medium” shipment cost case below. Figure 4 shows for five counties the demand and the number of open PODs over time under an eight-week quarantine (see §11 of the online supplement for the demand and number of open PODs over time under the no intervention case). Under both no intervention and eight-week quarantine, the number of open PODs starts to increase earlier than demand does. Because the opening and closing costs are only incurred once, when the demand at a location is expected to increase, a nearby POD is opened in advance to utilize the benefits of shipping from a nearby POD. This is mainly due to comparable shipment and facility operating costs. When fixed operating costs dominate the shipment costs, the number of open facilities closely follows the demand curve. Finally, in proportion to the number of infections, most of the PODs are operated in densely populated counties.

Figure 5(a) shows the average number of major facilities operated in each county. The major facilities in the densely populated DeKalb and Cobb counties

**Figure 5** Average Number of Open Major Facilities and Minimum, Average, and Maximum Durations PODs Are Open

are operated during almost the entire planning horizon serving the needs of these two counties as well as partially serving 13 surrounding counties.

Figures 5(b) and 5(c) show the minimum, average, and maximum open durations for the PODs in each county. The minimum open duration of the PODs is higher in the quarantine case because of the smoother demand curve that lasts for a longer time. In the no intervention case, some of the PODs are opened when the demand peaks, and then they are closed when the demand decreases. The variability in the open durations of the PODs is higher in densely populated counties (e.g., Cobb, DeKalb, Fulton, and Gwinnett) because the demand curves of these counties demonstrate higher peaks, increasing the number of openings and closings.

## 7. Conclusions and Future Directions

In this paper, we construct models for planning a food distribution network addressing facility location and resource allocation decisions during an influenza pandemic. We develop and utilize a disease spread model with a spatial and age-based structure for influenza pandemic and use this model for preparedness planning and testing intervention strategies. With the goal of planning food distribution during an influenza pandemic, we link the disease spread model to a facility location and resource allocation model. Using the disease spread model, we (dynamically) estimate the demand for food and provide it as an input to the facility location and resource allocation model. Since the corresponding facility location problem (CMF) is hard to solve for large instances, we design efficient algorithms (single-period add-drop heuristic, single-period hybrid heuristic, and single-period optimal heuristic) to find near-optimal solutions. Our computational results indicate that the single-period hybrid heuristic performs better than the single-period add-drop heuristic, but for very large instances that cannot be handled by commercial optimization software, the single-period add-drop heuristic is the best alternative. Using the heuristic algorithms developed for CMF, we propose two solution approaches, namely, the static approach (STAT) and the dynamic update approach (DYN), for the combined disease spread and facility location model. In STAT, the spread of disease and the demand for food are estimated only at the beginning of the planning horizon, and the food distribution network is constructed according to this estimate. In DYN, the estimates of disease spread and the food distribution facility location and resource allocation decisions are updated over time. We envision that a combined demand diffusion and resource allocation approach, such as the one proposed in this paper, could be useful in other applications, e.g., using a Bass diffusion model (Bass 1969) for demand and allocating limited resources for the manufacturing, marketing, and distribution of products.

We compare both STAT and DYN against the initial policies proposed by the ARC-MAC and illustrate the potential benefits of epidemiological and logistical modeling. We test the robustness of the proposed solution approaches and their variants through univariate and multivariate sensitivity analysis. We observe that DYN demonstrates a better response to the inaccuracies in the disease parameter estimates compared to STAT in terms of total cost and demand satisfaction. However, estimating disease parameters accurately, especially  $R_0$  and the durations of the exposed, presymptomatic, and symptomatic stages, is still important for DYN, especially if the facility-related opening, operating, and closing costs comprise a large portion of the total cost. A variant

of STAT, where a high  $R_0$  is assumed intentionally to build “excess capacity” (and account for parameter uncertainty), performs close to DYN in terms of demand satisfaction, but at the expense of significantly higher costs and workforce requirements (due to the higher number of facilities operated). Finally, another version of DYN that requires less frequent updates regarding the spread of the disease demonstrates a slight increase in unsatisfied demand and total cost in most cases. Whereas models such as STAT, which uses estimates from earlier influenza pandemics, can be used for advance planning purposes, adaptive and responsive approaches such as DYN that generate updated demand estimates after the pandemic begins are very useful in implementing response plans.

We study voluntary quarantine as an intervention policy and find the best timing and length of quarantine for different  $R_0$  values. Although the effect of quarantine on the IAR is limited, it can decrease the peak prevalence significantly, which is crucial for the continuity of the supply chains of goods and services. Quarantine can also reduce the probability of capacity problems in various industries during an influenza pandemic. For example, in the food distribution supply network, the number of facilities operated decreases by almost half in the case of a quarantine when compared to the no intervention case. This significant reduction demonstrates several benefits, including reduced equipment and workforce requirements for operating food distribution facilities where the workforce at each point in time is likely to be a scarce resource due to illness, fear of infection, and the need to care for infected family members. In addition to reducing the peak prevalence, quarantine delays the timing of the peak, which is also important because a delayed peak offers more time for preparedness efforts. These benefits would also apply to health services (Rahmandad and Sterman 2008). The results of our research have been incorporated into the ARC-MAC manual on food distribution planning during an influenza pandemic (American Red Cross 2008).

Fortunately, the most recent H1N1 pandemic in 2009 was not severe, and designing large distribution networks to satisfy the various needs of the public was not needed. However, the continuous mutation of the virus still poses a pandemic threat. Our results illustrate the potential benefits of detailed planning in response to a severe pandemic and the need for accurate modeling and analysis of spread of the disease.

In this paper, we focus on planning food distribution during an influenza pandemic. Designing vaccine and other medicine distribution supply chains and analyzing the effects of an influenza pandemic on the supply chain disruptions of various goods (e.g., milk,



gas) are other important problems that need to be considered when developing efficient response plans. When considering the distribution supply chain of medicines and vaccines, the decisions made during each time period affect the spread of the disease (and may decrease the number of infected people as well as the amount of food needed) and, thus, the decisions in future periods. A future direction is optimizing intervention policies such as the distribution of vaccines and antivirals. In our disease spread model, we do not assume any seasonal effects or viral evolution, which may change the spread pattern of the disease and is the focus of parallel work (Shi et al. 2010).

### Supplemental Material

Supplemental material to this paper is available at <http://dx.doi.org/10.1287/msom.2013.0460>.

### Acknowledgments

Special thanks to Joseph T. Wu of the University of Hong Kong for generously sharing his C++ code for the basic disease spread model and Randeep Ramamurthy for his help in the implementation of the disease spread model. The authors thank Marilyn Self from the American Red Cross Metropolitan Atlanta Chapter, Garry McGiboney from the Georgia Department of Education, and Pat O'Neal from the Georgia Department of Human Resources for insightful discussions and a synergistic collaboration. The authors also thank editor-in-chief Stephen C. Graves, the associate editor, and the four anonymous referees for their constructive comments. Support for this research was provided by the following Georgia Tech benefactors: Andrea Laliberte, Joseph C. Mello, the Nash Family, Claudia L. and J. Paul Raines, and Richard "Rick" E. and Charlene Zalesky.

### References

- American Red Cross (2006) Pandemic influenza preparedness and response plan (draft). Metropolitan Atlanta Chapter, American Red Cross, Atlanta.
- American Red Cross (2008) Food planning for pandemic flu project plan (draft). Metropolitan Atlanta Chapter, American Red Cross, Atlanta.
- Ballou RH (1968) Dynamic warehouse location analysis. *J. Marketing Res.* 5(3):271–276.
- Bass FM (1969) A new product growth model for consumer durables. *Management Sci.* 15(5):215–227.
- Canel C, Khumawala BM, Law J, Loh A (2001) An algorithm for the capacitated, multi-commodity multi-period facility location problem. *Comput. Oper. Res.* 28(5):411–427.
- Carrat F, Pelat C, Levy-Bruhl D, Bonmarin I, Lapidus N (2010) Planning for the next influenza H1N1 season: A modelling study. *BMC Infectious Diseases* 10:301.
- Centers for Disease Control and Prevention (2012) First H3N2 variant virus infection reported for 2012. Accessed August 30, 2012, <http://www.cdc.gov/flu/spotlights/h3n2v-variant-utah.htm>.
- Chan M (2009) World now at the start of 2009 influenza pandemic. Statement to the press by WHO Director-General Dr. Margaret Chan, June 11, 2009. [http://www.who.int/mediacentre/news/statements/2009/h1n1\\_pandemic\\_phase6\\_20090611/en/](http://www.who.int/mediacentre/news/statements/2009/h1n1_pandemic_phase6_20090611/en/).
- Chin TDY, Foley JF, Doto IL, Gravelle CR, Weston J (1960) Morbidity and mortality characteristics of Asian strain influenza. *Public Health Rep.* 75(2):149–158.
- Cooper L (1964) Heuristic methods for location-allocation problems. *SIAM Rev.* 6(1):37–53.
- Culler L, Keller H (2010) Resident interactions at mealtime: An exploratory study. *Eur. J. Ageing* 7(3):189–200.
- Dimitrov NB, Goll S, Hupert N, Pourbohloul B, Meyers LA (2011) Optimizing tactics for use of the U.S. antiviral strategic national stockpile for pandemic influenza. *PLoS ONE* 6(1):e16094.
- Erlenkotter D (1981) A comparative study of approaches to dynamic location problems. *Eur. J. Oper. Res.* 6(2):133–143.
- Feldman E, Lehrer FA, Ray TL (1966) Warehouse location under continuous economies of scale. *Management Sci.* 12(9):670–684.
- Ferguson NM, Cummings DAT, Fraser C, Cajka JC, Cooley PC, Burke DS (2006) Strategies for mitigating an influenza pandemic. *Nature* 442(7101):448–452.
- Ferguson NM, Keeling MJ, Edmunds WJ, Gani R, Grenfell BT, Anderson RM, Leach S (2003) Planning for smallpox outbreaks. *Nature* 425(6959):681–685.
- Ferguson NM, Cummings DAT, Cauchemez S, Fraser C, Riley S, Meeyai A, Iamsirithaworn S, Burke DS (2005) Strategies for containing an emerging influenza pandemic in Southeast Asia. *Nature* 437(7056):209–214.
- Flahault A, Vergu E, Coudeville L, Grais RF (2006) Strategies for containing a global influenza pandemic. *Vaccine* 24(44–46): 6751–6755.
- Fung IC-H, Antia R, Handel A (2012) How to minimize the attack rate during multiple influenza outbreaks in a heterogeneous population. *PLoS ONE* 7(6):e36573.
- Gale J (2008) Flu pandemic may cost world economy up to \$3 trillion. Accessed September 30, 2012, <http://www.bloomberg.com/apps/news?pid=newsarchive&sid=ashmCPWATNwU>.
- Geoffrion AM, Graves GW (1974) Multicommodity distribution system design by Benders decomposition. *Management Sci.* 20(5):822–844.
- Germann TC, Kadau K, Longini IM, Macken CA (2006) Mitigation strategies for pandemic influenza in the United States. *Proc. Natl. Acad. Sci. USA* 103(15):5935–5940.
- Grais RF, Ellis JH, Glass GE (2003) Assessing the impact of airline travel on the geographic spread of pandemic influenza. *Eur. J. Epidemiology* 18(11):1065–1072.
- Hansen E, Day T (2011) Optimal antiviral treatment strategies and the effects of resistance. *Proc. Roy. Soc. B* 278(1708):1082–1089.
- Harmon K (2011) What will the next influenza pandemic look like? *Scientific American* (September 19), <http://www.scientificamerican.com/article.cfm?id=next-influenza-pandemic&page=3>.
- Heesterbeek JAP (2002) A brief history of  $R_0$  and a recipe for its calculation. *Acta Biotheoretica* 50(3):189–204.
- Hindi KS, Basta T (1994) Computationally efficient solution of a multiproduct, two-stage distribution-location problem. *J. Oper. Res. Soc.* 45(11):1316–1323.
- Hinojosa Y, Puerto J, Fernández FR (2000) A multiperiod two-echelon multicommodity capacitated plant location problem. *Eur. J. Oper. Res.* 123(2):271–291.
- Holmes EC, Taubenberger JK, Grenfell BT (2005) Heading off an influenza pandemic. *Science* 309(5737):989.
- Homeland Security Council (2007) National strategy for pandemic influenza: Implementation plan—One year summary, July 2007. <http://www.flu.gov/planning-preparedness/federal/pandemic-influenza-oneyear.pdf>.
- Hormozi AM, Khumawala BM (1996) An improved algorithm for solving a multiperiod facility location problem. *IIE Trans.* 28(2):105–114.
- Jacquez JA (1972) *Compartmental Analysis in Biology and Medicine: Kinetics of Distribution of Tracer-Labelled Materials* (Elsevier, Amsterdam).
- Kuehn AA, Hamburger M (1963) A heuristic program for locating warehouses. *Management Sci.* 9(4):643–666.

- Lam EHY, Cowling BJ, Cook AR, Wong JYT, Lau MSY, Nishiura H (2011) The feasibility of age-specific travel restrictions during influenza pandemics. *Theoret. Biol. Medical Model.* 8(1):44–57.
- Larson RC (2007) Simple models of influenza progression within a heterogeneous population. *Oper. Res.* 55(3):399–412.
- Lee BY, Brown ST, Korch GW, Cooley PC, Zimmerman RK, Wheaton WD, Zimmer SM, et al. (2010) A computer simulation of vaccine prioritization, allocation, and rationing during the 2009 H1N1 influenza pandemic. *Vaccine* 28(31):4875–4879.
- Lipsitch M, Cohen T, Cooper B, Robins JM, Ma S, James L, Gopalakrishna G, et al. (2003) Transmission dynamics and control of severe acute respiratory syndrome. *Science* 300(5627):1966–1970.
- Longini IM, Nizam A, Xu S, Ungchusak K, Hanshaworakul W, Cummings DA, Halloran ME (2005) Containing pandemic influenza at the source. *Science* 309(5737):1083–1087.
- Mills CE, Robins JM, Lipsitch M (2004) Transmissibility of 1918 pandemic influenza. *Nature* 432(7019):904–906.
- Morse SS, Garwin RL, Olsiewski PJ (2006) Next flu pandemic: What to do until the vaccine arrives? *Science* 314(5801):929.
- Narula SC, Ogbu UI (1979) An hierarchical location-allocation problem. *Omega* 7(2):137–143.
- Ohio Department of Health and Ohio Food Industry Foundation (2006) Pandemic influenza preparedness guide for retail food establishments. Ohio Department of Health and Ohio Food Industry Foundation, Columbus.
- Patel R, Longini IM, Halloran ME (2005) Finding optimal vaccination strategies for pandemic influenza using genetic algorithms. *J. Theoret. Biol.* 234(2):201–212.
- Rahmandad H, Sterman J (2008) Heterogeneity and network structure in the dynamics of diffusion: Comparing agent-based and differential equation models. *Management Sci.* 54(5):998–1014.
- Robelen EW (2009) Swine flu disruption has school officials looking for lessons. *Ed. Week* 28(31):12.
- Rvachev L, Longini IM (1985) A mathematical model for the global spread of influenza. *Math. Biosciences* 75(1):3–22.
- Shi P, Keskinocak P, Swann J, Lee B (2010) Modeling seasonality and viral mutation to predict the course of an influenza pandemic. *Epidemiology Infection* 138(10):1472–1481.
- Shulman A (1991) An algorithm for solving dynamic capacitated plant location. *Oper. Res.* 39(3):423–436.
- Smith DJ (2006) Predictability and preparedness in influenza control. *Science* 312(5772):392–394.
- Sweeney DJ, Tatham RL (1976) An improved long run model for multiple warehouse location. *Management Sci.* 22(7):748–758.
- Trust for America's Health (2009) Pandemic flu preparedness: Lessons from the frontlines. Accessed May 30, 2009, <http://healthyamericans.org/assets/files/pandemic-flu-lesson.pdf>.
- U.S. Census Bureau (2000) Census 2000 gateway. Accessed November 30, 2008, <http://www.census.gov/main/www/cen2000.html>.
- Van Roy TJ, Erlenkotter D (1982) A dual-based procedure for dynamic facility location. *Management Sci.* 28(10):1091–1105.
- Viboud C, Grais RF, Lafont BA, Miller MA, Simonsen L, for the Multinational Influenza Seasonal Mortality Study Group (2005) Multinational impact of the 1968 Hong Kong influenza pandemic: Evidence for a smoldering pandemic. *J. Infectious Diseases* 192(2):233–248.
- Viboud C, Bolle P, Cauchemez S, Lavenue A, Valleron A, Flahault A, Carrat F (2004) Risk factors of influenza transmission in households. *British J. General Practice* 54(506):684–689.
- Wallinga J, Teunis P, Kretzschmar M (2006) Using data on social contacts to estimate age-specific transmission parameters for respiratory-spread infectious agents. *Amer. J. Epidemiology* 164(10):936–944.
- World Health Organization (2005) Avian influenza: Assessing the pandemic threat. Accessed November 30, 2008, [http://whqlibdoc.who.int/hq/2005/WHO\\_CDS\\_2005.29.pdf](http://whqlibdoc.who.int/hq/2005/WHO_CDS_2005.29.pdf).
- World Health Organization (2012) Global alert and response. Accessed August 30, 2012, <http://apps.who.int/csr/disease/influenza/pandemic/en/index.html>.
- World Health Organization Writing Group (2006) Nonpharmaceutical interventions for pandemic influenza, national and community measures. *Emerging Infectious Diseases* 12(1):88–94.
- Wu JT, Riley S, Fraser C, Leung GM (2006) Reducing the impact of the next influenza pandemic using household-based public health interventions. *PLoS Medicine* 3(9):1532–1540.